Journal of Organometallic Chemistry 830 (2017) 167–174

Contents lists available at ScienceDirect

Journal of Organometallic Chemistry

journal homepage: www.elsevier.com/locate/jorganchem

Ruthenium complexes bearing a tridentate polypyridyl ligand with non-coordinating donor atoms: Construction of a specific coordination environment involving noncovalent interactions

Dai Oyama [a], [*], Takashi Yamanaka [a], Ryosuke Abe [a], Tsugiko Takase [b]

[a] Department of Industrial Systems Engineering, Cluster of Science and Engineering, Fukushima University, 1 Kanayagawa, Fukushima, 960-1296, Japan
[b] Institute of Environmental Radioactivity, Fukushima University, 1 Kanayagawa, Fukushima, 960-1296, Japan

ARTICLE INFO

Article history:
Received 28 June 2016
Received in revised form
14 November 2016
Accepted 2 December 2016
Available online 3 December 2016

Keywords:
Carbonyl ligands
Ligand effects
Noncovalent interactions
Ruthenium
X-ray diffraction
Polypyridine

ABSTRACT

We have prepared carbonyl (CO) ruthenium complexes which contained the tridentate polypyridyl type ligand (2,6-di(1,8-naphthyridin-2-yl)pyridine; dnp) with non-coordinating nitrogen atoms, for the development of specific reactions using noncovalent interactions. Similar to the aqua precursors that display intramolecular hydrogen bonds between the aqua and dnp ligands, a noncovalent interaction is formed between the terminal carbonyl ligand and non-coordinating nitrogen atoms of dnp; its strength depends on the identity of the axial ligand (triphenylphosphine or pyridine). Additionally, we investigated the reactivity of dnp-containing complexes bearing carbonyl ligands in both the equatorial and axial positions. As a result, it is suggested that the noncovalent interaction between dnp and CO ligands in positions equatorial to the dnp ligand is relatively strong, because the axial carbonyl ligand dissociates preferentially in ligand substitution reactions using organic solvents. Furthermore, in the ligand substitution reaction with a nitrile derivative, the coordination space constructed by the $\{Ru\text{-}dnp\}^{2+}$ unit enables regulation of not only the ligand substitution reaction rate but also the identity of the donor atom. The present complex also leads to activation and cleavage of inert C—Cl and C—Br bonds.

1. Introduction

The study of high molecular selectivity based on molecular design has proven to be a particularly promising area of research in coordination chemistry. When chemists develop molecular designs, they often refer to the active sites of metalloproteins which create precise reaction spaces and strictly control biochemical reactions. The ability of metalloproteins to regulate their coordination spaces has been studied using a number of model compounds, and numerous energetic studies have been undertaken, e.g. the stabilization of small molecules utilizing intramolecular hydrogen bonds by picket fence and hangman porphyrin complexes as heme-based molecules [1,2] or by tripodal pyridyl complexes as nonheme-based molecules [3].

We have synthesized aqua ruthenium complexes that contained the tridentate polypyridyl-based ligand (2,6-di(1,8-naphthyridin-2-yl)pyridine; dnp) which has multiple non-coordinating nitrogen atoms [4]. As a preliminary study in this series, we examined the intramolecular hydrogen bonds between the nitrogen atoms of dnp and aqua ligand. When the axial ligand was triphenylphosphine (PPh_3; $[\mathbf{1a}]^{2+}$ in Scheme 1), a single hydrogen bond was formed between OH_2 and dnp. On the contrary, two hydrogen bonds were formed when the axial ligand was pyridine (py) ($[\mathbf{1b}]^{2+}$). Consequently, it was found that the complex system could control some reactivities, such as the rate constant (k_{obs}) of the aqua substitution reaction and the acid dissociation constant (pK_a) [4]. In addition, since dnp has two 1,8-naphthyridyl units at the 2- and 6-positions of the central pyridyl ring, the coordination space in the equatorial plane is narrower than that of the prototype, 2,2′:6′,2″-terpyridine (tpy). Therefore, it was also suggested that the dnp structure led to selective coordination of entering ligands by limiting the available coordination space [5].

In this study, novel ruthenium complexes containing a carbonyl ligand (*trans*(A)-$[Ru(dnp)(CO)A_2]^{2+}$; A = PPh_3 ($[\mathbf{2a}]^{2+}$) or py ($[\mathbf{2b}]^{2+}$)) were prepared to explore noncovalent interactions other than hydrogen bonding. Similar to $[\mathbf{1}]^{2+}$, the axial ligands (PPh_3 and py) may affect the strength of the interaction between the carbonyl and the dnp ligand in $[\mathbf{2}]^{2+}$. Furthermore, to investigate the

---

[*] Corresponding author.
E-mail address: daio@sss.fukushima-u.ac.jp (D. Oyama).

http://dx.doi.org/10.1016/j.jorganchem.2016.12.001

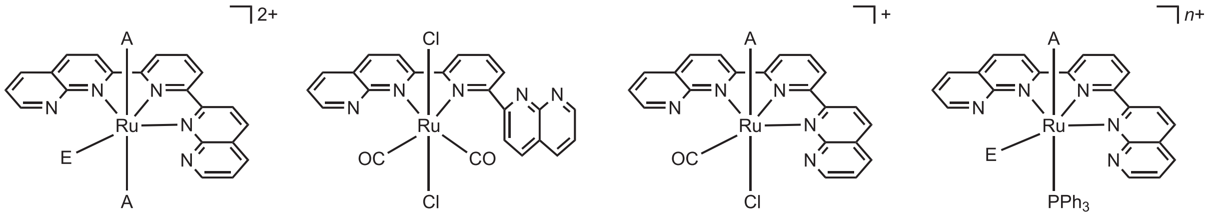

$[\mathbf{1a}]^{2+}$: E = OH_2, A = PPh_3
$[\mathbf{1b}]^{2+}$: E = OH_2, A = py
$[\mathbf{2a}]^{2+}$: E = CO, A = PPh_3
$[\mathbf{2b}]^{2+}$: E = CO, A = py

[**3a**]

$[\mathbf{3b}]^{+}$: A = CO
$[\mathbf{4a}]^{+}$: A = Me_2SO
$[\mathbf{4b}]^{+}$: A = Me_2CO
$[\mathbf{4c}]^{+}$: A = MeCN

$[\mathbf{5a}]^{2+}$: E = $ClCH_2CN$, A = PPh_3
$[\mathbf{5b}]^{+}$: E = OH_2, A = Cl

Scheme 1. Ru-dnp complexes presented in this study.

strength of the noncovalent interaction between the coordinated carbonyl and dnp ligands, we synthesized a dicarbonyl complex containing carbonyl ligands in both the equatorial and axial positions relative to the dnp ligand ($[Ru(dnp)(CO)_2Cl]^+$; $[\mathbf{3b}]^+$). This complex was prepared via an intermediate ([**3a**]) containing the bidentate dnp ligand. Using $[\mathbf{3b}]^+$, ligand substitution reactions were carried out in some organic solvents. The results suggested that the noncovalent interaction between the equatorial CO and dnp was significantly strong. In addition, another ligand substitution reaction involving a chlorinated nitrile derivative was also carried out to examine ligand selectivity based on the coordination space of dnp in $[\mathbf{1}]^{2+}$. Activation and cleavage of carbon–halogen bonds was observed when the reactions were heated.

2. Experimental

2.1. Physical measurements

Elemental analysis data were obtained on a Perkin Elmer 2400II series CHN analyzer (Yokohama, Japan). ^1H, $^{13}C\{^1H\}$, and $^{31}P\{^1H\}$ NMR spectra (298 K) were recorded on a JEOL JMN-AL300 spectrometer (Tokyo, Japan) operating at the ^1H, ^{13}C, and ^{31}P frequencies of 300, 75.5, and 121 MHz, respectively. Electrospray ionization mass spectrometry (ESI-MS) data were obtained on a Bruker Daltonics micrOTOF (Yokohama, Japan). Infrared spectra were obtained as KBr pellets with a JASCO FT-IR 4100 spectrometer (Tokyo, Japan). Electronic absorption spectra were obtained in 1 cm quartz cuvettes on a JASCO V-570 UV/VIS/NIR spectrophotometer (Tokyo, Japan). Electrochemical measurements were performed on an ALS/Chi model 660E electrochemical analyzer (Tokyo, Japan). Electrochemical measurements of complexes were performed in CH_3CN containing tetrabutylammonium perchlorate (TBAP, 0.1 M) as a supporting electrolyte in a one-compartment cell comprising a platinum working electrode, platinum wire counter electrode, and a $Ag/AgNO_3$ (0.01 M in CH_3CN) reference electrode. All potentials are reported in Volts versus the ferrocenium/ferrocene couple (Fc^+/Fc) at 298 K under Ar. Kinetic measurements for substitution reactions were carried out at 313(1) K in a constant temperature water bath. Absorption spectra were recorded at the appropriate intervals. A_f was measured when the absorbance had stopped changing. Values of the pseudo-first-order rate constants (k_{obs}) were obtained from the slopes of the plots of $\ln(A_f - A_t)$ against time [6]. Photoreactions of the complexes were conducted in Ar-sparged solvents. The solutions were irradiated with visible light ($\lambda > 400$ nm) through a cutoff filter using an Asahi Spectra MAX-302 (Tokyo, Japan) fitted with a xenon lamp (25 mW cm^{-2}). The ground state, gas-phase structures of $[\mathbf{2a}]^{2+}$, $[\mathbf{2b}]^{2+}$, and $[\mathbf{3b}]^+$ were optimized using density functional theory (DFT) calculations at the B3LYP level [7]. The LanL2DZ basis set was used for the ruthenium atom [8]. The 6-31G(d) basis set was employed for the other atoms [9]. No imaginary frequencies were obtained when frequency calculations on optimized geometries were performed. All calculations were performed using the Gaussian 09W program package [10].

2.2. Preparation of complexes

All chemicals were used without further purification unless otherwise noted. All solvents purchased for synthesis were anhydrous and were used without further purification. Acetonitrile for electrochemical measurements was purified using a Glass Contour Ultimate Solvent System. Carbon monoxide gas (99.95%) was purchased from Japan Fine Products. Ruthenium trichloride was purchased from Furuya Metal Co., Ltd. The syntheses of 2,6-di(1,8-naphthyridin-2-yl)pyridine (dnp), $[Ru(CO)_2Cl_2]_n$, and aqua complexes ($[\mathbf{1a}]^{2+}$ and $[\mathbf{1b}]^{2+}$) have been previously reported [4,11,12].

2.2.1. *$[Ru(dnp)(PPh_3)_2(CO)](PF_6)_2$ ($[\mathbf{2a}](PF_6)_2$) and $[Ru(dnp)(py)_2(CO)](PF_6)_2$ ($[\mathbf{2b}](PF_6)_2$)*

A solution of $[\mathbf{1a}](PF_6)_2$ (100 mg, 0.079 mmol) in 2-methoxyethanol (60 mL) was heated at 100 °C under an atmosphere of carbon monoxide (10 atm) for 16 h. After some insoluble matter was removed by filtration, the volume of the filtrate was reduced to 10 mL using a rotary evaporator. Addition of diethyl ether to the solution resulted in the formation of $[\mathbf{2a}](PF_6)_2$ as an orange precipitate. The product was collected by filtration, washed with diethyl ether and dried in vacuo. The crude product was recrystallized from acetonitrile/diethyl ether. Yield: 86 mg (85%). Anal. calcd. for $[Ru(dnp)(PPh_3)_2(CO)](PF_6)_2$: $C_{57}H_{43}N_5OF_{12}P_4Ru$: C 54.47, H 3.39, N 5.48, found: C 54.42, H 3.58, N 5.34%; ESI-MS (CH_3CN): *m/z* 494.7 ($[M]^{2+}$), 349.6 ($[M-(CO)-(PPh_3)]^{2+}$); IR (KBr): 2003 cm^{-1} (νCO); ^1H NMR (CD_3CN): $\delta = 9.45$ (dd, $J = 4.5$, 1.8 Hz, 2H), 8.41–8.29 (m, 7H), 7.96 (d, $J = 8.8$ Hz, 2H), 7.88 (dd, $J = 7.8$, 4.1 Hz, 2H), 7.16 (t, $J = 7.4$ Hz, 6H), and 6.89–6.74 (m, 24H) ppm; $^{13}C\{^1H\}$ NMR (CD_3CN): $\delta = 159.67$, 156.38, 155.52, 154.18, 142.66, 141.19, 139.75, 133.30, 133.23, 133.15, 131.51, 131.49, 129.10, 129.03, 128.97, 128.90, 128.60, 128.29, 127.99, 126.93, 125.85, and 122.11 ppm; $^{31}P\{^1H\}$ NMR (CD_3CN): $\delta = 32.92$ ppm. Using a protocol similar to that described for the synthesis of $[\mathbf{2a}](PF_6)_2$, the reaction between $[\mathbf{1b}](PF_6)_2$ (100 mg, 0.11 mmol) and CO gas (15 atm) gave $[\mathbf{2b}](PF_6)_2$ in 75% yield (76 mg). Anal. calcd. for $[Ru(dnp)(py)_2(CO)](PF_6)_2$: $C_{32}H_{23}N_7OF_{12}P_2Ru$: C 42.12, H 2.54, N 10.74, found: C 41.93, H 2.44, N 10.98%; ESI-MS (CH_3CN): *m/z* 260.5 ($[M-2(py)+2(N_2)]^{2+}$), 246.5 ($[M-2(py)-(CO)+2(N_2)]^{2+}$); IR (KBr): 2017 cm^{-1} (νCO); ^1H NMR (CD_3CN): $\delta = 9.43$ (dd, $J = 4.5$, 1.8 Hz, 2H), 8.87 (t, $J = 8.4$ Hz, 4H), 8.71–8.59 (m, 5H), 7.96 (dd, $J = 8.4$, 4.5 Hz, 2H), 7.80